REPORT DOCUMENTATION PAGE	*Form Approved* *OMB No. 0704-0188*

1. REPORT DATE *(DD-MM-YYYY)*	2. REPORT TYPE	3. DATES COVERED *(From - To)*
01-12-2005	Book Chapter	

4. TITLE AND SUBTITLE	5a. CONTRACT NUMBER
Velocity and Transport Characteristics of the Louisiana-Texas Coastal Current	
	5b. GRANT NUMBER
	5c. PROGRAM ELEMENT NUMBER 0602435N
6. AUTHOR(S) Jarosz, Ewa, Murray, Stephen P.	5d. PROJECT NUMBER
	5e. TASK NUMBER
	5f. WORK UNIT NUMBER 73-6643-B5-5

7. PERFORMING ORGANIZATION NAME(S) AND ADDRESS(ES)	8. PERFORMING ORGANIZATION REPORT NUMBER
Naval Research Laboratory Oceanography Division Stennis Space Center, MS 39529-5004	NRL/BC/7330-05-5141
9. SPONSORING/MONITORING AGENCY NAME(S) AND ADDRESS(ES)	10. SPONSOR/MONITOR'S ACRONYM(S) ONR
Office of Naval Research 800 N. Quincy St. Arlington, VA 22217-5660	11. SPONSOR/MONITOR'S REPORT NUMBER(S)

12. DISTRIBUTION/AVAILABILITY STATEMENT

Approved for public release, distribution is unlimited.

13. SUPPLEMENTARY NOTES U.S. Government authors; Jarosz; Murray

14. ABSTRACT

The Louisiana-Texas Coastal Current (LTCC) is a major dynamic feature responsible for the distribution of fresh water, sediment and nutrients on the northwestern shelf of the Gulf of Mexico. Earlier studies have indicated that this current exhibits a distinct although asymmetric annual cycle during which it flows downcoast, i.e., westward along the Louisiana coast and then southward along the Texas coast in fall, winter, and spring; however, in summer, the flow reverses and moves upcoast. This annual cycle of the LTCC is clearly observed with measurements from a cross-shore current meter mooring array located south of Cameron, LA in 1996 and 1997. Analyses of these data show that the currents are indeed downcoast between September 1996 and January 1997 with modest mean velocities up to 6 cm/s. During the expected upcoast regime of June-August 1996, our data show mean eastward speeds of 2-6cm/s. Cross-shelf spatial correlation length scales of the currents are well in excess of 60km during the downcoast regime but they are distinctly smaller (30-50 km) during the upcoast regime. Coherence analysis and predictions from a wind-driven model indicate that the downcoast currents and volume transport associated with them are highly coherent with alongshore wind stress. This wind stress also controls fluctuations of the upcoast currents and transport; however, it is not a dominant forcing. The data indicate that during the analyzed summer season, the alongshore sea-surface slope was also an important driving force of the LTCC.

15. SUBJECT TERMS

Louisiana-Texas Coastal Current (LTCC), downcoast, upcoast, wind-driven model, sea-surface slope

16. SECURITY CLASSIFICATION OF: a. REPORT	b. ABSTRACT	c. THIS PAGE	17. LIMITATION OF ABSTRACT	18. NUMBER OF PAGES	19a. NAME OF RESPONSIBLE PERSON
Unclassified	Unclassified	Unclassified	UL	14	Ewa Jarosz
					19b. TELEPHONE NUMBER *(Include area code)* 228-688-4292

Standard Form 298 (Rev. 8/98)
Prescribed by ANSI Std. Z39.18

20060605024

PUBLICATION OR PRESENTATION RELEASE REQUEST

Pubkey: 4404

NRLINST 5600.2

1. REFERENCES AND ENCLOSURES	2. TYPE OF PUBLICATION OR PRESENTATION	3. ADMINISTRATIVE INFORMATION
Ref: (a) NRL Instruction 5600.2 (b) NRL Instruction 5510.40D Encl: (1) Two copies of subject paper (or abstract)	( ) Abstract only, published ( ) Book ( ) Conference Proceedings (refereed) ( ) Invited speaker ( ) Journal article (refereed) ( ) Oral Presentation, published ( ) Other, explain ( ) Abstract only, not published (X) Book chapter ( ) Conference Proceedings (not refereed) ( ) Multimedia report ( ) Journal article (not refereed) ( ) Oral Presentation, not published	STRN NRL/BC/7330-05-5141 Route Sheet No. 7330/ Job Order No. 73-6643-B5-5 Classification X U ___ C Sponsor ONR BASE approval obtained X yes ___ no

4. AUTHOR

Title of Paper or Presentation

Velocity and Transport Characteristics of the Louisana-Texas Coastal Current

Author(s) Name(s) (*First,MI,Last*), Code, Affiliation if not NRL

Ewa Jarosz (Dr), S. P. Murray

It is intended to offer this paper to the ______________________________

(*Name of Conference*)

____

(*Date, Place and Classification of Conference*)

and/or for publication in **Circulation in the Gulf of Mexico, Unclassified** ______________________________

(*Name and Classification of Publication*) (*Name of Publisher*)

After presentation or publication, pertinent publication/presentation data will be entered in the publications data base, in accordance with reference (a).

It is the opinion of the author that the subject paper (is ____) (is not X) classified, in accordance with reference (b).

This paper does not violate any disclosure of trade secrets or suggestions of outside individuals or concerns which have been communicated to the Laboratory in confidence. This paper (does ____) (does not X) contain any militarily critical technology.

This subject paper (has ____) (has never X) been incorporated in an official NRL Report.

Ewa Jarosz (Dr), 7332 — Ewa Jarosz

Name and Code (*Principal Author*) (Signature)

5. ROUTING/APPROVAL

CODE	SIGNATURE	DATE	COMMENTS
Author(s) Jarosz	Ewa Jarosz		Need by 25-Feb-05 Publicly accessible sources used for this publication
Section Head Hwang	Paul A Hwang	2/3/05	
Branch Head **Robert A Arnone, 7330**	R Arnone	2/7/05	
Division Head Capt. Garrett ~~Ruth H. Preller~~, 7300 acting	R.P. Garrett	2/3/05	1. Release of this paper is approved. 2. To the best knowledge of this Division, the subject matter of this paper (has ____) (has never X) been classified.
Security, Code **7030.1**	David K. Anderson	2/10/05	1. Paper or abstract was released. 2. ~~A copy is filed in this office.~~ SSC-85-5
Office of Counsel, Code **1008.3**	Armand A. Beck	2/8/2005	
ADOR/Director NCST **E.O. Hartwig, 7000**			
Public Affairs (*Unclassified/ Unlimited Only*), Code **7030.4**	Shirley Rotunda	2/7/05	
Division, Code			
Author, Code			

HQ-NRL 5511/6 (Rev. 12-98) (e) THIS FORM CANCELS AND SUPERSEDES ALL PREVIOUS VERSIONS

Velocity and Transport Characteristics of the Louisiana-Texas Coastal Current

Ewa Jarosz[1] and Stephen P. Murray[2]

Coastal Studies Institute, Louisiana State University, Baton Rouge, Louisiana, USA

The Louisiana-Texas Coastal Current (LTCC) is a major dynamic feature responsible for the distribution of fresh water, sediment and nutrients on the northwestern shelf of the Gulf of Mexico. Earlier studies have indicated that this current exhibits a distinct although asymmetric annual cycle during which it flows downcoast, i.e., westward along the Louisiana coast and then southward along the Texas coast in fall, winter, and spring; however, in summer, the flow reverses and moves upcoast. This annual cycle of the LTCC is clearly observed with measurements from a cross-shore current meter mooring array located south of Cameron, LA in 1996 and 1997. Analyses of these data show that the currents are indeed downcoast between September 1996 and January 1997 with modest mean velocities up to 6 cm/s. During the expected upcoast regime of June–August 1996, our data show mean eastward speeds of 2–6 cm/s. Cross-shelf spatial correlation length scales of the currents are well in excess of 60 km during the downcoast regime but they are distinctly smaller (30–50 km) during the upcoast regime. Coherence analysis and predictions from a wind-driven model indicate that the downcoast currents and volume transport associated with them are highly coherent with alongshore wind stress. This wind stress also controls fluctuations of the upcoast currents and transport; however, it is not a dominant forcing. The data indicate that during the analyzed summer season, the alongshore sea-surface slope was also an important driving force of the LTCC.

INTRODUCTION

The Mississippi River is the major source of fresh water, sediment, nutrients, and pollutants for the northern shelf of the Gulf of Mexico. It drains 42% of the continental watershed of the United States and has an annual average discharge rate of ~ 19,000 m^3/s [*Wiseman et al.*, 1997]. The outflow usually peaks in spring and is at a minimum in early fall. The river enters the Gulf of Mexico through the Mississippi River birdfoot delta and the Atchafalaya River, which is a distributary of the Mississippi River diverted from the main channel at Old River, north of Baton Rouge, LA. Thirty percent of the total discharge is delivered to the Louisiana shelf by the Atchafalaya River. The remaining seventy percent flows through the Mississippi River delta. Recent estimates, however, suggest that only 43% of the fresh water discharged by the birdfoot delta is carried to the western Louisiana shelf [*Etter et al.*, 2004]. This portion of the Mississippi River outflow joins with the Atchafalaya River discharge, mixes with the shelf waters and ultimately forms a coastal current [*Wiseman and Kelly*, 1994; *Murray et al.*, 1998]. The coastal flow has been called various names in

[1]Now at Oceanography Division, Naval Research Laboratory, Stennis Space Center, Mississippi, USA.
[2]Now at Office of Naval Research, Arlington, Virginia, USA.

Circulation in the Gulf of Mexico: Observations and Models
Geophysical Monograph Series 161

10.1029/161GM11

the literature: for instance, it was referred to as the Louisiana Coastal Current by *Wiseman and Kelly* [1994] and the Texas current by *Vastano et al.* [1995]. The latest studies [*Murray et al.*, 1998; *Nowlin et al.*, 1998] show that despite strong spatial and temporal variability, this current can generally be traced west of the Mississippi River delta along the entire Louisiana and Texas coasts. Therefore it seems reasonable to refer to it as the Louisiana-Texas Coastal Current (LTCC).

During much of the year, the LTCC flows westward along the shore from Louisiana to Texas, consistent with a balance between the cross-shelf pressure gradient set up by the river and the local Coriolis force. This may suggest that the flow is in general agreement with geostrophic theory and is driven mainly by the pressure gradient. In such a scenario the river outflow is deflected to the right upon entering the sea (the Gulf of Mexico) in the northern hemisphere, producing a buoyant coastal current trapped against the coastline. Observations and analyses do not, however, support such a simple behavior of the LTCC. *Smith* [1975, 1978] reports seasonal variability of the current on the central Texas shelf with a strong south-southwesterly flow in winter and weak north-northeasterly or south-southwesterly flow in summer. He also implies that many features of the nearshore current pattern can be explained as a response to surface wind stress. *Crout et al.* [1984] also describe seasonal variability of the current on the western Louisiana inner shelf, and conclude that the summer current is generally disorganized and probably driven by nonlocal forcing. In contrast to the summer flow, the winter alongshore current is better organized and is well correlated with alongshore wind stress. Similar conclusions regarding the wind stress and winter flow are drawn by *Wiseman et al.* [1986]. *Cochrane and Kelly* [1986], synthesizing previous investigations, report that alongshore wind stress is the major driving force of the coastal current on the Louisiana-Texas shelf in a region west of 92.5°W. During much of the year (usually from September through May), the current flows downcoast (in the sense of Kelvin wave phase propagation in the northern hemisphere), and is highly correlated with the downcoast wind stress component. In late summer, there is a reversal of the flow direction and upcoast flow, well correlated with the wind, prevails. The summer upcoast flow was observed as far east as 90.5°W [*Jarosz*, 1997]. Based on hydrographic and current meter data analyses, this annual reversal of the nearshore circulation on the northern shelf of the Gulf of Mexico and its dependence on the alongshore wind stress is also reported by *Li et al.* [1997], *Murray et al.* [1998] , *Nowlin et al.*, [1998], *Cho et al.*, [1998], *Nowlin et al.* [2005], and *Walker* [2005]. The asymmetric annual cycle of the nearshore circulation is also well reproduced by numerical models [*Oey*, 1995; *Current*, 1996; *Zavala-Hidalgo et al.*, 2003]. Additionally, *Murray et al.* [1998] showed that during the summer upcoast flow regime, current fluctuations in southern Texas are significantly coherent with the alongshore sea-surface slope and wind stress; however, variability of the current in central Texas and central Louisiana is highly coherent primarily with the alongshore sea-surface slope.

In contrast to the larger scale resolution of the previous studies, this paper utilizes a data set from a current meter array specifically deployed to study cross-shore variability and coherence at one location in the LTCC [*Murray et al.*, 2001]. We focus on the variability of currents and volume transport observed within the LTCC on the Louisiana inner shelf west of both the Atchafalaya and Mississippi deltas (approximately along the 93°W longitude line). Our primary objective is to use the current meter data from the cross-shore array (a) to determine the seasonal cycle of the mean flow in the LTCC and its fluctuations in different seasons, i.e. in summer (upcoast regime) and fall/winter (downcoast regime), (b) to estimate the correlation between the LTCC currents and alongshore wind stress in this region, and (c) to estimate the transport of the LTCC and its seasonal variability as well as its dependence on driving mechanisms such as wind stress, sea-surface slope and buoyancy forcing as represented by the Atchafalaya River discharge.

DATA

A map of the Louisiana-Texas shelf (Figure 1) shows the locations where the observations were collected for this work: (a) the inner-shelf transport resolving array off Cameron, LA, (b) subsurface pressure gauges, and (c) anemometer locations. The type of a current meter available to this study was the ducted impeller Endeco Model 174, which employs a tether line to filter out surface wave velocities and allows the instrument to orient in the mean flow direction. Our data, though obtained with an instrument array lacking the vertical resolution of an ADCP current meter, still provide significant new insight into the characteristics of the LTCC. Table 1 gives the location and total water depth at each mooring along with the relative depth of each current meter, distance from the coast for each location and time coverage of the current observations. Note the mooring array extends over 65 km in the cross-shore direction, from about the 10-m isobath to the 22-m isobath, over a fairly uniformly sloping bottom. The location for the transport array was selected based on two considerations: (a) to be far enough downstream from the Atchafalaya River mouth to escape its direct influence and the influence of the large Tiger and Trinity shoals located just west of the river mouth; and (b) survivability, since any mooring in the water column on the Louisiana inner shelf will survive oil industry traffic and fishing pressure only if it

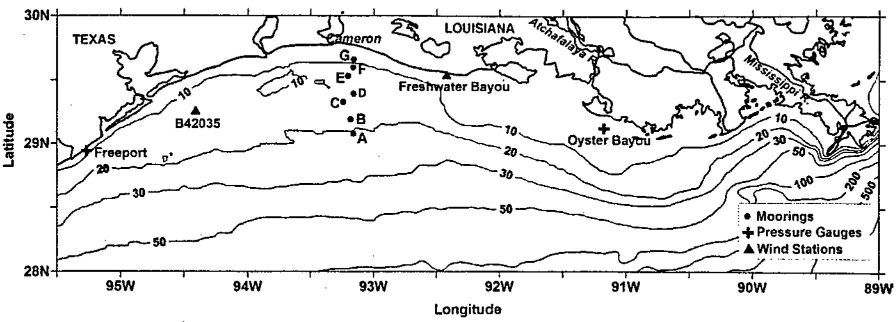

Figure 1. Regional map containing study transect (A through G moorings) of the LTCC south of Cameron, LA. Pressure gauges at Oyster Bayou and Freeport, and wind stations at Freshwater Bayou and the US buoy off Galveston (B42035) are also shown.

is located near an existing oil field structure (in our case usually a standpipe). We selected standpipes and small platforms (1–10 m in diameter) and placed the moorings 2–3 diameters from them on a line as near to a coastal normal as possible. The outer mooring is located on the 22-m isobath, and, as repeated high-resolution hydrographic sections (with a station spacing of approximately 7 km) in this region [*Murray et al.*, 1998] have shown, this distance from the coast would usually capture the lower salinity waters except during the summer upcoast flow regime when the low salinity waters spread farther offshore.

Equipment malfunctions and severe weather limited the data return in the 1995 pilot program, but better instrumentation deployed in May 1996 greatly improved data returns (see Table 1 for time coverage of this deployment) [*Murray et al.*, 2001]. A period extending from May 1996 to April 1997 conveniently allows the study of the two distinct flow regimes: the upcoast (summer) flow regime of 1996 (a period between 1 June and 14 August 1996) and the downcoast (fall/winter) flow regime of 1996–97 (a period between 26 September 1996 and 4 January 1997). The time period analyzed for the upcoast flow regime begins in June, in a month when

Table 1. Mooring configurations.

Mooring	Longitude(W)	Latitude(N)	Total Depth (m)	Instrument Depth (m)	Distance Offshore (km)	Start Time–Stop Time
Atop[1)]	93.16277°	29.08033°	23.1	7.8	76.92	05/14/1996–09/19/1996
Amid[1)]				13.3		05/14/1996–09/19/1996
Btop[2)]	93.18233°	29.19233°	19.5	5.5	64.45	09/07/1996–04/16/1997
Bmid[2)]				10.0		09/07/1996–04/16/1997
Ctop[1,2)]	93.24219°	29.3289°	17.7	6.4	49.54	05/13/1996–09/11/1997 09/19/1996–04/16/1997
Cmid[1,2)]				11.0		05/13/1996–09/11/1996 09/19/1996–01/18/1997
Cbot[1,2)]				15.0		05/13/1996–09/11/1996 09/19/1996–01/18/1997
Dtop[1)]	93.243°	29.39167°	15.0	5.5	40.85	05/30/1996–09/19/1996
Etop[1,2)]	93.20417°	29.53033°	13.1	5.7	27.06	05/30/1996–08/31/1996 09/25/1996–01/24/1997
Ebot[2)]				10.0		09/25/1996–01/14/1997
Ftop[1,2)]	93.16433°	29.59967°	12.0	6.5	19.79	05/13/1996–06/18/1996 09/06/1996–01/05/1997
Fbot[1,2)]				10.0		05/13/1996–06/18/1996 09/06/1996–01/05/1997
Gtop[1)]	93.16084°	29.66033°	10.0	5.5	13.40	05/14/1996–08/27/1996

[1)] Instruments used for upcoast regime analyses; [2)] instruments used for downcoast regime analyses.

the LTCC usually changes its direction from downcoast to upcoast, and it ends one day before a strong cold front, normally observed during the downcoast flow regime, moved through the mooring array. The time duration for the downcoast flow regime encompasses the longest common time period with good data return from the analyzed instruments. Additionally, the numbers adjacent to each current meter in Table 1 indicate which instruments are used in the summer (^{1}) and fall/winter (^{2}) flow regime studies.

Our intent here is to describe only the subinertial variability (below 0.6 cpd); therefore all analyses presented in the subsequent sections used low-pass-filtered data with a cutoff frequency of 0.6 cpd (Butterworth filter). Additionally, all quantities are referred to a Cartesian coordinate system (x, y, z) with x positive eastward (upcoast), y positive northward (onshore), and z positive upward.

MEANS AND VARIABILITY OF THE CURRENTS

Figure 2 shows the variations of means at various depths as a function of distance from the shore for both current components and flow regimes. Additionally, Table 2 lists these means as well as standard deviations, root-mean-square errors of the means estimated as suggested by *Kundu and Allen* [1976], major axis orientations of the velocity variance, and orientations of the mean flow.

An examination of the means and mean flow orientations clearly shows two different patterns, i.e., in the summer of 1996, the mean flow was directed eastward (upcoast) at all considered locations at speeds between 2–6 cm/s, while the direction of the flow was westward (downcoast) throughout the water column in the fall and winter of the 1996–97 season with speeds up to approximately 6 cm/s. This annual cycle of the inner shelf circulation is also apparent in progressive vector diagrams (Plate 1). These diagrams show eastward displacement for the summer and persistent downcoast movement during the fall/winter season. The magnitude of the mean flow when examined at different distances offshore for the same regime does not show much variability for flows recorded at similar depths. There is, however, a noticeable decrease in magnitude of the net displacement and alongshore means with increasing depth, especially evident for the downcoast regime (Plate 1b and Table 2). On inner shelves, i.e., in shallow water regions, where surface and bottom boundary layers typically overlap and interact with each other, and the currents usually align with the direction of forcing, this weakening of the mean flow with depth could probably be attributed to a decreasing influence of surface forcing with depth as well as to bottom friction. Additionally, only one out of 17 estimated cross-shelf velocity means (Table 2) is statistically significant at the 95% significance level. Thus we conclude that the means of the cross-shelf component do not show any clear pattern in the analyzed seasons.

The large standard deviations (Table 2), usually 2–3 times larger than the means, and the meandering of the flow clearly visible in Plate 1 document the significant current variability in the LTCC during both upcoast and downcoast regimes.

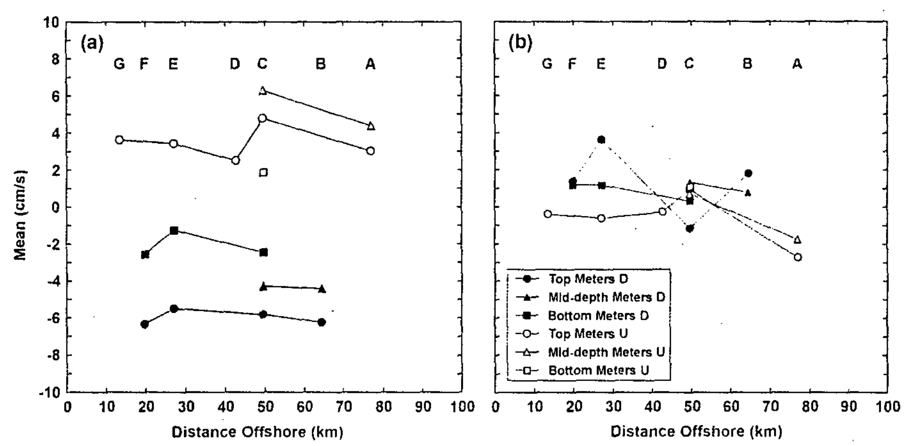

Figure 2. Means of (a) the alongshore (east-west) and (b) cross-shore (north-south) current components for the upcoast (open symbols) and downcoast (solid symbols) flow regimes; positive values are upcoast (eastward) and onshore (northward) for the alongshore and cross-shore means, respectively.

Table 2. Mooring statistics.

Mooring	$\bar{u}$ (cm/s)	$\bar{v}$ (cm/s)	u_{SD} 1) (cm/s)	v_{SD} 1) (cm/s)	u_{SE} 2) (cm/s)	v_{SE} 2) (cm/s)	Major Principle Axis (deg) 3,4)	Mean Flow Orientation (deg) 3)
				Upcoast Regime				
Atop	3.0	-2.7	14.1	12.6	6.6	6.6	51	132
Amid	4.4	-1.8	11.8	8.9	5.5	3.7	65	112
Ctop	4.8	0.9	10.3	5.8	2.5	1.5	93	79
Cmid	6.3	0.7	8.4	5.8	1.7	1.1	90	84
Cbot	1.9	1.1	3.1	3.5	0.6	0.6	30	60
Dtop	2.5	-0.3	8.5	6.8	1.6	1.7	80	97
Etop	3.4	-0.6	8.2	5.7	1.7	1.2	91	100
Gtop	3.6	-0.4	8.8	3.4	1.9	0.6	93	96
				Downcoast Regime				
Btop	-6.2	1.8	13.5	5.0	2.4	1.2	86	286
Bmid	-4.4	0.8	12.0	5.9	2.1	0.9	90	280
Ctop	-5.8	-1.2	10.0	3.7	1.7	0.4	88	259
Cmid	-4.3	1.3	11.1	4.8	1.8	0.7	84	287
Cbot	-2.4	0.3	8.2	4.8	1.3	0.7	70	277
Etop	-5.5	3.6	10.9	4.8	1.6	0.6	101	304
Ebot	-1.2	1.2	5.9	3.3	0.9	0.4	93	314
Ftop	-6.3	1.4	14.7	4.8	2.3	0.5	98	282
Fbot	-2.6	1.2	9.3	3.3	1.3	0.5	91	295

1) Standard deviations of respective current components; 2) rms errors of mean estimates; 3) measured clockwise from true north; 4) 180° ambiguity should be added.

From Table 2 it is also apparent that the alongshore standard deviation u_{SD} consistently decreases with depth, whereas the cross-shore standard deviation v_{SD} remains nearly constant with depth for both summer and fall/winter seasons. As one approaches the coast, there is also a decreasing trend for both standard deviations in summer, while nearly constant values in the same direction are found for the fall/winter period. rthermore, the fluctuations during the downcoast season are anisotropic ($u_{SD} > v_{SD}$) and their principle direction is almost east-west, as is the direction of local isobaths and coastline. During the upcoast season, however, the fluctuation field is more isotropic ($u_{SD} \approx v_{SD}$), especially near the bottom and at the moorings located farther offshore. Nearer to the shore, these fluctuations again follow the direction of local isobaths. Additionally, large standard deviations usually imply large standard errors of the means (Table 2) uggesting that the mean flow speeds are not statistically different from 0. Thus one may conclude that the mean currents in the Gulf of Mexico off Cameron, LA were very sluggish, especially in summer 1996.

SPATIAL CORRALATIONS OF THE CURRENTS IN THE LTCC

An inspection of the raw data as well as the progressive ector diagrams (Plate 1) suggest that the currents are visibly correlated at the different depths and locations. To determine whether this visual observation is valid, the complex correlation coefficient [*Kundu*, 1976], whose magnitude gives the overall measure of correlation between two current records, was computed separately for the upcoast and downcoast flow regimes. The magnitudes of this coefficient for the top instruments as a function of a mooring separation distance are displayed in Figure 3. Using the algorithm for a confidence level estimation suggested by *Sciremammano* [1979], coefficients greater than 0.29 for the downcoast flow and 0.33 for the upcoast flow are significant at the 95% confidence level.

It is very apparent from Figure 3 that the cross-shore spatial correlation length scale of the currents within the LTCC is different for downcoast and upcoast flows. For the downcoast regime, the magnitude of the complex correlation coefficient is in the 0.86–0.91 range and varies little across the mooring array. Such high values suggest that the cross-shore spatial length scale of the flow is undoubtedly much larger than the maximum available separation distance, i.e., it is larger than 60 km, and our mooring array is not resolving this scale well in the fall/winter season. In contrast, magnitudes of the correlation coefficients found for the upcoast regime are smaller, and, for instance, their value at the 50-km separation distance reaches only 0.32 in the summer season as opposed to 0.89 in the fall/winter period. Additionally, the

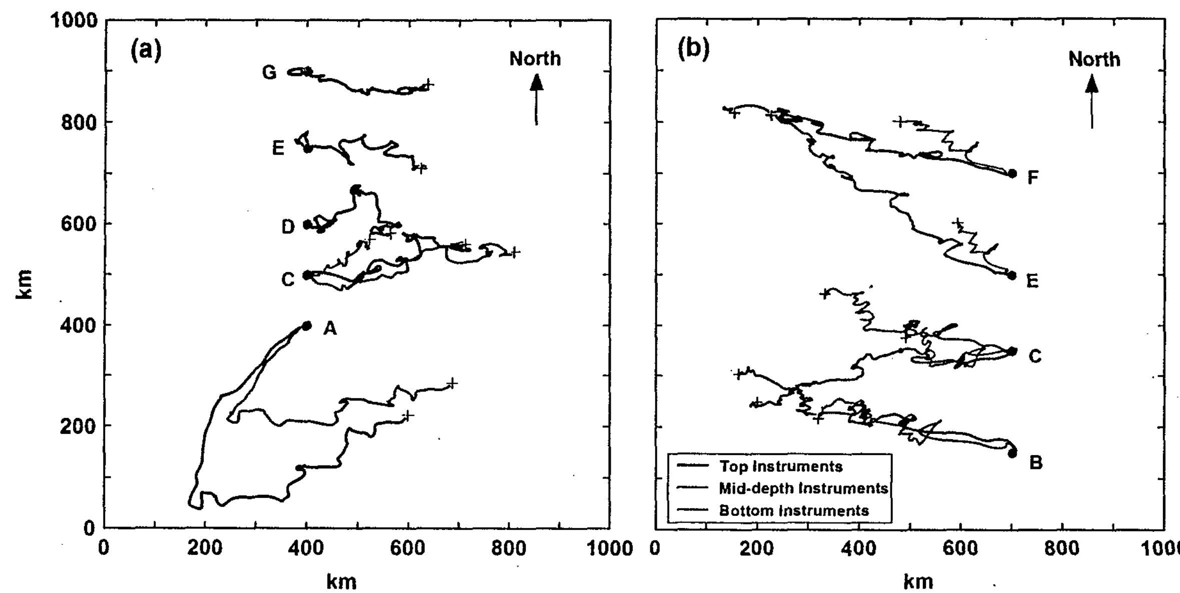

Plate 1. Progressive vectors diagrams for (a) the upcoast and (b) downcoast flow regime; depths are color-coded and offset for clarity; the solid red circles mark the initial position; the red pluses mark the final position.

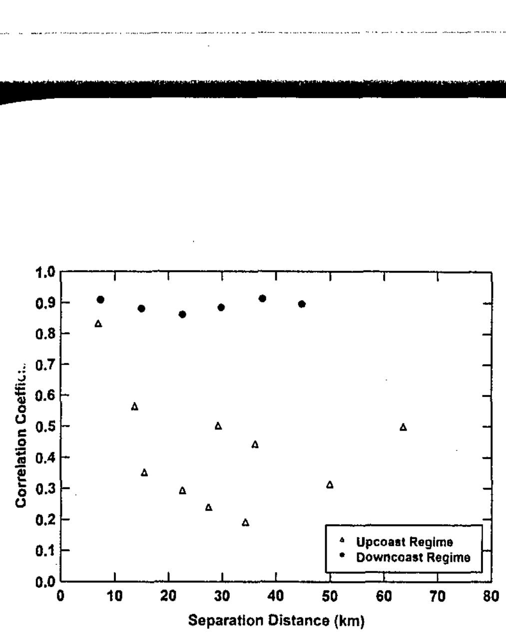

Figure 3. Correlation coefficients as a function of the cross-shore separation distance for the upcoast (open triangles) and downcoast (solid circles) flow regimes; the coefficients are computed only for the top instruments.

summer coefficient does not display a monotonic decrease with increasing separation distance as often observed in other coastal regions [*Kundu and Allen*, 1976; *Dever*, 1997]. However, inspection of the correlation values and their errors suggest that the summer cross-shore spatial length scale could be between 30 km and 50 km.

The distinct difference in spatial length scales of the LTCC currents between seasonal regimes may result from differences in the scale and strength of forcing mechanisms such as winds [*Gutiérrez de Velasco and Winant*, 1996; *Wang et al.*, 1998]. During the downcoast regime, the spatial length scale is much larger than 60 km, meaning that it is greater than the width of the LTCC (48 km as estimated by *Murray et al.* [1998]). This large spatial scale probably results from coherence imposed on the surface layer by the large and energetic synoptic scale weather systems (cold fronts) impacting the northern Gulf of Mexico in fall, winter, and spring. These systems usually induce strong vertical mixing and drive flows inside and outside of the LTCC with similar efficiency [*Wiseman et al.*, 1986; *Wiseman and Kelly*, 1995; *Murray et al.*, 1998]. In summer, more complicated spatial structure of the coastal current, its weaker and more variable speed, smaller scale forcing generated by less organized and weaker winds and/or well-developed stratification could be partly responsible for the much shorter cross-shelf spatial length scale.

There is also a difference between values of the correlation coefficients of the upcoast and downcoast regimes as a function of vertical separation (results not shown). The correlation coefficients are high (> 0.8) in both regimes for adjacent instruments and drop to approximately 0.54 for the summer season and to 0.75 for the fall/winter time period for larger vertical separations (9 m or more). The weaker correlation of the summer currents at the separation distance of 9 m or more could be related to summer stratification. The well-developed summer pycnocline is able to isolate effectively flow observed in the lower layer of the water column from direct forcing such as winds, for example. Consequently, the flow in the lower layer is usually very weak, disorganized and often opposed to the flow observed above the pycnocline [*Crout et al.*, 1983; *Murray et al.*, 1998]. The relationship between currents at different depths strengthens significantly due to weaker stratification in fall/winter months and deeper influence of wind forcing.

VELOCITY CEOFS

To extract variability that is coherent across the mooring array and quantify major patterns in the LTCC currents, we subjected the data to complex empirical orthogonal function analysis (CEOF) [*Kundu and Allen*, 1976]. For each flow regime, the velocity CEOFs were computed by forming a matrix containing demeaned complex velocities obtained from the low-frequency along- and cross-shore current components for all available depths in a given season. Complex eigenvectors estimated from the associated covariance matrix were then converted into amplitudes and veering angles for each statistically significant mode (Table 3). The amplitudes of each mode were also scaled by the square root of the corresponding eigenvalue, and the veering angles were relative to the Btop and Atop currents for the downcoast and upcoast flows, respectively.

For the fall/winter months, only the first CEOF mode is statistically significant when tested with an algorithm proposed by *North et al.* [1982]. It explains 81.1% of the current variability, and its spatial structure shows very little variation in veering angles in the Cameron cross-section (Table 3). The spatial distribution of the amplitudes and veering angles suggests that the primary downcoast flow pattern is in a form of a surface-intensified coastal jet. The first mode is also highly correlated with the alongshore wind stress with a squared correlation coefficient (R^2) of 0.73 that is significant at the 95% confidence level. This high correlation clearly shows that the alongshore wind stress is an important driving mechanism of the LTCC fluctuations in the downcoast flow regime. Additionally, dominance of the first mode and its high correlation with the wind stress suggest that this mode represents a predominant barotropic response of the inner shelf current to the strong fall/winter winds and storms. Plate 2 demonstrates how swiftly the currents respond to changes in the alongshore wind stress forcing. This plate shows daily values of wind stress (Plate

Table 3. Amplitudes[1] (cm/s) and veering angles[2] (deg) of the CEOF modes.

Downcoast Regime			Upcoast Regime				
Mooring	Amp 1	Angle 1	Mooring	Amp 1	Dir 1	Amp 2	Dir 2
Btop	13.1	0	Atop	12.4	0	6.9	0
Bmid	12.1	356	Amid	10.4	3	5.1	27
Ctop	8.7	356	Ctop	5.8	341	8.8	163
Cmid	11.1	358	Cmid	6.1	331	6.5	167
Cbot	8.4	344	Cbot	2.3	279	1.5	154
Etop	10.6	352	Dtop	6.8	349	6.2	172
Ebot	5.2	3	Etop	4.1	357	0.6	255
Ftop	14.0	8	Gtop	5.3	357	0.9	159
Fbot	8.5	2					

[1]Amp 1 and Dir 1 are amplitudes and veering angles of mode 1; Amp 2 and Dir 2 are amplitudes and veering angles of mode 2. [2] Veering angles are relative to currents measured at Btop and Atop moorings for the downcoast and upcoast regimes, respectively.

2a) and combined mean flow and mode 1 for each mooring on 6 and 9 October 1996 (Plates 2b and 2c, respectively). On 6 October, a wind stress of 0.11 Pa was directed downcoast as were the currents across the entire Cameron section. On 7 October, this downcoast stress started diminishing and on 8 October, changed direction to upcoast. The currents followed these changes in wind stress. On 9 October, the downcoast flow stopped and at most locations, the flow began to move upcoast as shown in Plate 2c. Similar behavior of the currents in the fall/winter/spring months on the Louisiana-Texas inner shelf, i.e., their swift response to the wind stress variations, is reported by *Murray et al.*, [1998].

For the upcoast current data, CEOF modes 1 and 2 are the only statistically significant modes. Mode 1 is not as dominant as in the downcoast flow, but it can explain 46% of the flow variance, while mode 2 accounts for 25% of the variance. The amplitudes of these modes are smaller and the veering angles vary more (especially those of mode 2) than those of mode 1 estimated from the downcoast data. The angles of summer mode 2 imply two current reversals occurring (a) offshore (between moorings A and C) and (b) near the coast (between moorings E and G) (Table 3). Additionally, the spatial structure of the amplitudes and veering angles of mode 1 suggest that one of the current patterns in summer could be a jet confined to the upper 10 to 14 m of the water column. This conclusion agrees with summer current observations collected on the Louisiana inner shelf and presented by *Murray et al.*, [1998]. The spatial structure of the second mode could represent more complex summer flow also described by *Murray et al.*, [1998]. Their ADCP, CTD measurements, and SCULP drifters [*Johnson and Niiler*, 1994; *Ohlmann et al.*, 2001] showed that in summer 1994, there were three distinct zones in the region where our moorings were later deployed namely (a) a coherent eastward flow of waters with salinity of 30 psu and higher, (b) an interior zone of slow, disorganized flow of intermediate salinity waters (20–30 psu), and (c) a near coastal westward flow of low salinity waters (less 20 psu).

In contrast to the high correlation between the currents and alongshore wind stress in the downcoast regime, the summer current fluctuations are not very correlated with this forcing. The squared correlation coefficient between summer CEOF mode 1 and the alongshore wind stress is low and its magnitude is 0.31 (R^2 greater than 0.12 is significant at the 95% confidence level which was computed from the algorithm proposed by *Sciremammano* [1979]), while there is no correlation between mode 2 and this component of the wind stress ($R^2 = 0.04$). The complex spatial structure of the coastal current, its highly variable speed, and or well-developed stratification could be partly responsible for the low correlation between the current and wind stress in summer.

A WIND-DRIVEN MODEL

To further clarify the role of local wind stress as a major force controlling current variability within the LTCC off Cameron, LA, a wind-driven model, previously used successfully to study variability of currents within the Amazon River coastal plume [*Lentz*, 1995], is employed. This model assumes that current variability is caused solely by wind stress. Thus the input of energy from the wind into the plume layer is balanced only by a constant linear friction at the base of the plume and the temporal acceleration of the alongshore flow. This alongshore momentum balance is expressed as followed:

$$\frac{\partial u}{\partial t} + \frac{ru}{h} = \frac{\tau_{sx}}{\rho h} \tag{1}$$

where u is the alongshore current, ρ is the reference water density, r is the linear friction coefficient, h is the plume thickness and τ_{sx} is the alongshore wind stress. Integrating (1) in time and solving for u yields

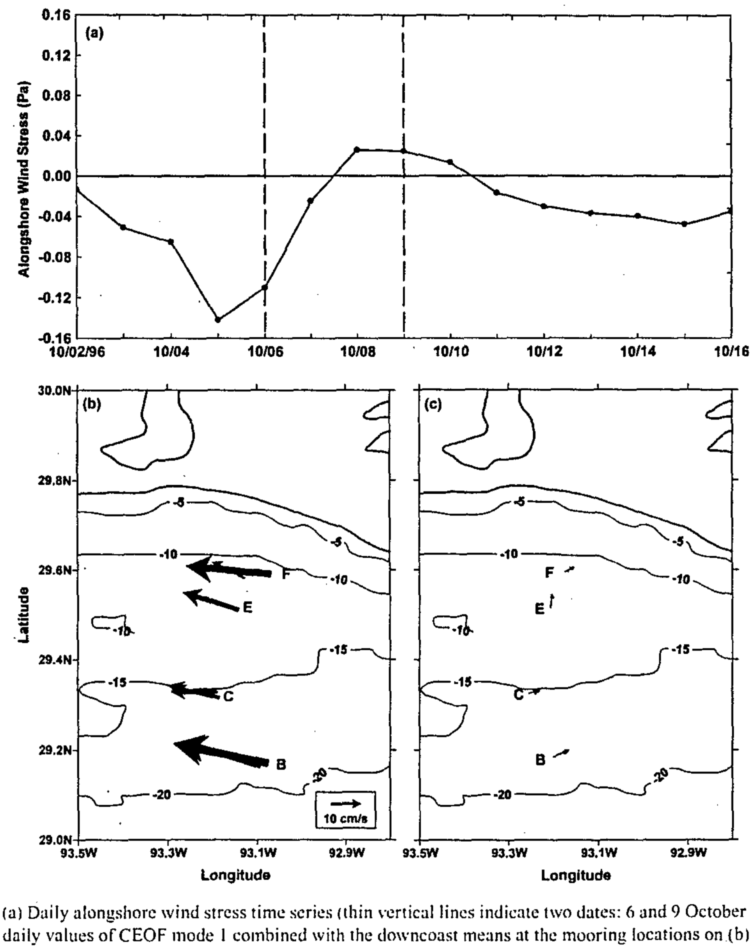

Plate 2. (a) Daily alongshore wind stress time series (thin vertical lines indicate two dates: 6 and 9 October 1996), and maps of daily values of CEOF mode 1 combined with the downcoast means at the mooring locations on (b) 6 October 1996 and (c) 9 October 1996; black, blue, and green arrows represent top, mid-depth, and bottom current meters, respectively. Positive values are upcoast (eastward).

$$u(t)=\int_0^t \frac{\tau_{sx}}{\rho h}\exp(-r(t-t')/h)dt'+u(t=0)\exp(-rt/h) \quad (2)$$

The alongshore wind stress component was computed from the wind data measured at Freshwater Bayou using the approach proposed by *Large and Pond* [1981]. As in *Lentz* [1995], the linear friction coefficient was chosen to yield the best agreement with the observations. For the downcoast flow regime, the alongshore current component was calculated from (2) at three different mooring locations (B, C and F), and then compared with the observations collected by the top meters at each locations. The best agreement between the wind-driven alongshore velocities based on (2) and the observed velocities is found at mooring F (Figure 4a), with h = 12 m and the reference density of 1021 kg/m^3. We used h equal to the total water depth in moorings F and G (data from mooring G were used for the upcoast regime computations presented in the next paragraph) because the historical hydrographic data suggested that the entire water column near these mooring locations was filled out with light waters (salinity less then 30 psu). The squared correlation coefficient between the observations and predictions with r = 0.0003 m/s is 0.66 (all correlations presented in this section are significant at the 95% confidence level computed from the algorithm proposed by *Sciremammano* [1979]). Variability of the predicted wind-driven alongshore current is very similar to that observed at F, for instance, events observed between 3 and 11 October 1996, 22 October and 4 November 1996, and 7 and 19 November 1996. Analogous conclusions are obtained for the other two moorings (mooring C: R^2 = 0.58; mooring B: R^2 = 0.58). These results reinforce the earlier conclusion that alongshore wind stress, which alone explains at least 58% of the current variance, is a dominant driving force of the current variability observed within the LTCC in the downcoast flow regime.

When the wind stress observed in the summer regime is applied to (2), amplitudes of the alongshore velocities are poorly modeled for almost entire June but they are quite well reproduced for July and August 1996. The model estimates are again compared with subsurface current observations at three different locations (moorings A, C, and G). The best agreement is found at mooring G (Figure 4b), with a squared correlation coefficient of 0.37 between the observed alongshore velocities and estimates, with r = 0.00035 m/s, h = 10 m, and the reference density of 1010 kg/m^3. It is obvious that major velocity fluctuations in July and August, particularly events observed between 1 and 6 August are wind driven. However, the predicted variability in June, still in transition from downcoast to upcoast dynamics, is different from the observations, with amplitude differences reaching even 30 cm/s, which is quite large because lower speeds are usually measured within the LTCC in summer. Similar conclusions are found when predictions are compared with subsurface

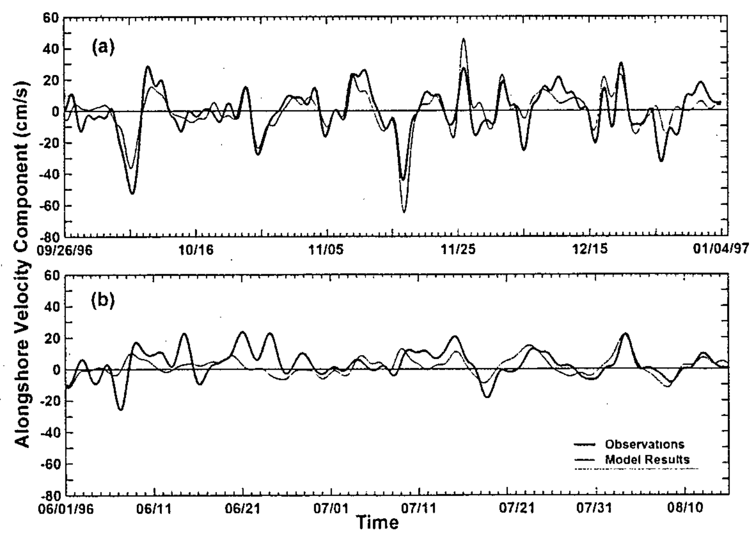

Figure 4. (a) The alongshore 6.5m current observed at mooring F during the downcoast flow regime and (b) the alongshore 5.5m current observed at mooring G during the upcoast flow regime compared to the model results (equation 2); positive values indicate upcoast velocities, while negative values indicate downcoast velocities.

currents at moorings C ($R^2 = 0.34$) and A ($R^2 = 0.32$). These results suggest that alongshore wind stress, explaining by itself as much as 37% of the current variance, is an important driving force of the coastal current in the upcoast flow regime. The unexplained variance of the currents implies that other driving forces, such as barotropic and baroclinic pressure gradients, could be also important in summer.

The friction coefficients used for the simulations of the LTCC currents are in the range of bottom friction coefficients estimated for the Louisiana-Texas inner shelf by *Chuang and Wiseman* [1983]. For both flow regimes, these friction coefficients are an order of magnitude larger than those utilized for the Amazon plume ($r = 0.00002$ m/s) [*Lentz*, 1995], and this magnitude difference is mainly due to the vertical size of the Amazon plume and Mississippi-Atchafalaya outflow at their respective locations. In the case of the Louisiana inner shelf, the low salinity waters at moorings F and G extend from the surface to the bottom, and the friction coefficient is simply the bottom friction coefficient, while it is the interlayer friction coefficient for the Amazon plume.

CROSS-SECTIONAL TRANSPORT

In order to calculate the transport within the LTCC through the section off Cameron, we first produce a time series of the low-passed alongshore current component at each current meter. The data are then interpolated onto a grid (1-m depth by 2-km cross-shore distance) at each hour, using linear interpolation. A rigorous definition of the offshore extent of the coastal current is obviously difficult because of its inherent temporal variability; however, the limited salinity data recovered from the moorings suggest the presence of coastal plume water across the section even as far out as mooring A. Thus we make an operational definition of the coastal current transport by integrating across the section between moorings A and G, recognizing that this estimate is a lower bound. It does, however, have the advantage of being consistent with the ship-mounted ADCP transport estimates of *Murray et al.* [1998].

The alongshore transport through the section during the downcoast regime of 1996–1997 is shown in Figure 5a. Note the persistent downcoast transport of -0.1 to -0.15 Sv with a record length mean of -0.06 Sv (a root-mean-squared error of 0.02 Sv). Significant bursts of elevated downcoast transport occur on 6 October, 17 November, and 8 and 13 January. We will examine the spatial characteristics of some of these bursts later. The corresponding transport during the preceding upcoast regime is shown in Figure 5b. As expected, regional forcing conditions in the summer of 1996 cause the coastal current to reverse directions, but it shifts predominantly upcoast by 9 June and remains upcoast for most of the summer. Note, however, the temporal variability

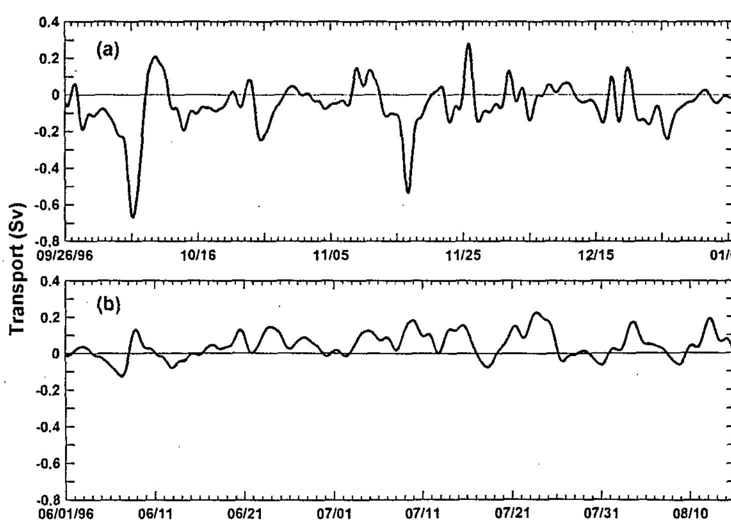

Figure 5. Transport in the LTCC during (a) the downcoast flow regime and (b) upcoast flow regime; positive values indicate the upcoast transport, while negative values indicate downcoast transport.

in the transport. These transport fluctuations, which range from slightly below 0 to maximums of 0.15 to 0.23 Sv, occur roughly on a 5-day time scale. The record length mean for this period is 0.05 Sv with a root-mean-squared error of 0.03 Sv. Our mean seasonal transport results are in surprisingly good agreement with results from a high-resolution (a 1/20° grid in latitude and longitude) NCOM model of the Gulf of Mexico driven with climatological monthly surface fluxes [*Zavala-Hidalgo et al.*, 2003, Figure 2A]. The model results for a section close to our observations, integrated from the 25 m isobath to the coast, show a 10-month transport of the downcoast flow reaching -0.1 Sv and a 2-month transport of the summer upcoast flow reaching approximately 0.04 Sv.

The most energetic transport oscillations during the fall/winter period appear closely related to direct wind driving, as seen during the event between 2 and 11 October (Figure 5a). Ten days of northeasterly winds exert downcoast wind stresses that produce downcoast current speeds in excess of 30 cm/s across the entire section with two zones of intensification (Plates 1b and 2b). A high-speed current (speeds of 60 cm/s) occupies the outer (southern) edge of the section, and a second jet, nearly as strong, occupies the inshore (northern) end of the section. Previous data taken during LATEX B cruises [*Murray et al.*, 1998] suggest that intense vertical mixing, combined with zones of intensified horizontal density gradients (fronts), are associated with these jets in the coastal current. The cessation of the northeasterly winds driving the October 6 intensification of the downcoast flow event is followed by an upcoast flow event.

The time series of transport during the summer regime (Figure 5b) is similarly characterized by fluctuations with several days to week time scales. The strongest upcoast intensification, centered on 23 July, is notable for its rather modest current speeds of 20 cm/s observed along the mooring array. These wind driven upcoast currents are upwelling favorable, leading to offshore transport in the surface layer and a consequent weakening of cross-shore density gradients and reduction of baroclinic alongshore velocities.

DRIVING FORCES OF THE LTCC

To seek further insight into dynamical relationships controlling the transport observed along the transect, we examined multiple and partial coherence between the transport and four forcing mechanisms: (a) alongshore wind stress, (b) cross-shore wind stress, (c) alongshore barotropic pressure gradient (a sea-surface slope), and (d) buoyancy forcing proxied by the river discharge as in *Münchow and Garvine* [1993]. Wind stress was computed from the anemometer at Fresh Water Bayou. The sea-surface slope was calculated from subsurface pressure gauges located at Oyster Bayou and Freeport for both seasons, and buoyancy forcing is represented by Atchafalaya River discharge.

Figure 6 shows multiple and partial coherence over the 0.05 to 0.6 cpd frequency band between the transport and possible driving mechanisms. For the fall/winter observation period (Figure 6a), 78% to 96% of the total transport fluctuations, shown by the multiple coherence curve, are explained by the four forcing variables. Looking at individual partial coherences, the alongshore wind stress clearly accounts for a majority (at least 65%) of the transport variance. There is also an indication that the cross-shore wind stress might be considered a significant forcing for the transport fluctuations with periods between 3 and 5 days. Partial coherences of the alongshore sea-surface slope and river discharge with the downcoast transport are rarely statistically significant, thus their importance as possible sources of subtidal transport fluctuations is extremely small, if any.

In the summer flow regime, 60% to 92% of the transport fluctuations (Figure 6b) are accounted for by the four possible driving forces over the entire frequency band examined. During this regime, the transport fluctuations are not only coherent with the alongshore wind stress, but also with the alongshore sea-surface slope at frequencies lower than 0.45 cpd. In addition, the cross-shore wind stress could be an important influence on the transport fluctuations with periods between 5 and 10 days, but its importance is clearly secondary compared to the alongshore wind stress and sea-surface slope. Partial coherence between the transport and buoyancy forcing represented by the Atchafalaya discharge only appears statistically significant for frequencies lower than 0.2 cpd, with the percentage of variance explained by this possible driving force reaching about 75% at 0.1 cpd.

SUMMARY AND CONCLUSIONS

Temporal and spatial variability of the currents and volume transport of the Louisiana-Texas Coastal Current were studied with data from a cross-shore transect located south of Cameron, Louisiana. In addition to the current meter data, subsurface pressure, wind, and the Atchafalaya River discharge were also analyzed to better understand the local behavior of the LTCC on the western Louisiana inner shelf. Two subsets of the data, one for the upcoast (summer) and another for the downcoast (fall/winter) flow regimes, were analyzed to determine whether there were any differences in the current characteristics and transport between these two regimes of the LTCC.

In the fall/winter season, the fluctuations of the currents and transport are highly dependent on the wind forcing. The overall mean flow is downcoast (westward) as expected for this part of a year; however, the rotating winds associ-

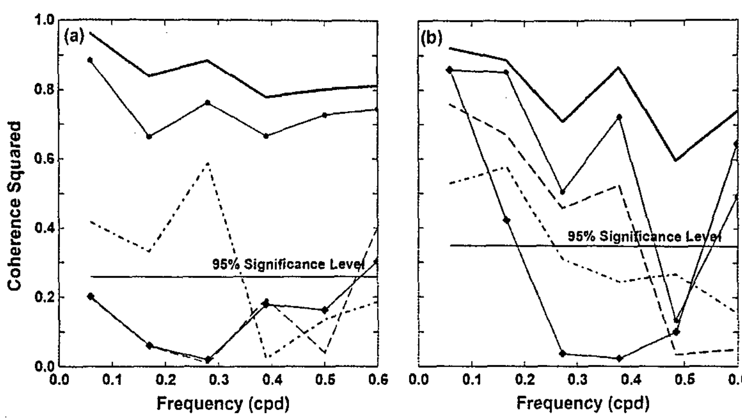

Figure 6. Multiple (thick line) and partial coherence (symbol lines) between the transport observed during (a) the downcoast regime and (b) the upcoast regime and alongshore wind stress (solid line with circles), cross-shore wind stress (dash-dot line), alongshore sea-surface slope (dashed line), and the Atchafalaya River discharge (solid line with diamonds); the lower straight solid line is the 95% significance level.

...ed with cold fronts do temporarily reverse its direction to upcoast (eastward) for 18–36 hours. The downcoast flow is clearly polarized in the alongshore direction. High correlations in the vertical and large cross-shore spatial length scale of the observed currents as well as the spatial structure of the amplitudes and veering angles of the dominant velocity CEOF mode (mode 1) strongly suggest a surface-intensified jet-like response to the wind forcing. Based on high correlation of the currents and transport with the alongshore wind ress, we conclude that this wind stress component is the principal driving mechanism of the LTCC off Cameron, LA during the downcoast flow, which is in agreement with the findings of other investigators [*Crout et al.*, 1984; *Cochrane and Kelly*, 1986; *Li et al.*, 1997; *Murray et al.*, 1998; *Cho et al.*, 1998; *Nowlin et al.*, 2005; *Walker*, 2005].

During the upcoast regime, vertical and cross-shore correlation length scales are markedly lower than during the downcoast regime. The mean flow as well as the mean transport is directed upcoast, but again with persistent fluctuations which are two to three times larger than the seasonal means. These fluctuations also become more isotropic with increasing depth and increasing distance off the coast than those observed in the fall/winter season. The current and transport variability is partly related to the alongshore wind stress; however, the correlation between this wind stress and both currents and their transport is weaker. Thus we conclude that other forcing mechanisms such as barotropic nd/or baroclinic pressure gradients could be important in summer. Our data indicate that during the analyzed summer season, in addition to the alongshore wind stress, the alongshore sea-surface slope was also an important driving forcing of the LTCC, which agrees with the conclusions reached by *Murray et al.* [1998].

Acknowledgments. This study was funded by the Minerals Management Service under contract 14-35-001-30724 awarded to Louisiana State University.

REFERENCES

Cho, K., R. O. Reid, and W. D. Nowlin Jr. (1998), Objectively mapped stream function fields on the Texas-Louisiana shelf based on 32 moored current meter data, *J. Geophys. Res., 103*, 10,377–10,390.

Chuang, W. S. and W. J. Wiseman, Jr. (1983), Coastal sea level response to frontal passages on the Louisiana-Texas shelf, *J. Geophys. Res., 88*, 2615–2620.

Cochrane, J. D., and F. J. Kelly (1986), Low-frequency circulation on the Texas-Louisiana shelf, *J. Geophys. Res. 91*, 10,645–10,659.

Crout, R. L., W. J. Wiseman, Jr., and W. S. Chuang (1984), Variability of wind driven currents, west Louisiana inner continental shelf: 1978-1979, *Contrib. Mar. Sci., 27*, 1–11.

Current, C. L. (1996), Spectral model simulation of wind driven subinertial circulation on the inner Louisiana-Texas Shelf, Ph.D. Thesis, 144 pp., Texas A&M University, Collage Station.

Dever, E. P. (1997), Subtidal velocity correlation scales on the northern California shelf, *J. Geophys. Res. 102*, 8555–8571.

Etter, P. C., M. K. Howard, and J. D. Cochrane (2004), Heat and freshwater budgets of the Louisiana – Texas shelf, *J. Geophys. Res., 109*, C02024, doi:10.1029/2003JC001820.

Gutiérrez de Velasco G., and C. D. Winant (1996), Seasonal patterns of wind stress and wind stress curl over the Gulf of Mexico, *J. Geophys. Res., 101*, 18,127-18140.

Jarosz, E. (1997), Summer flow regime on the Louisiana inner shelf, M.S. thesis, pp. 74.Louisiana State University, Baton Rouge.

Johnson, W. R. and P. P. Niiler (1994), SCULP drifter study in the Northern Gulf of Mexico, AGU Fall Meeting, O52C-8, San Francisco.

Kundu, P. H. (1976), A note on the Ekman veering observed near the ocean bottom, *J. Phys. Oceanog.*, *6*, 238–242.

Kundu, P. H., and J. S. Allen (1976), Some three-dimensional characteristics of low-frequency current fluctuations near Oregon coast, *J. Phys. Oceanogr.*, *6*, 181–199.

Large, W. G. and S. Pond (1981), Open ocean momentum flux measurements in moderate and strong winds, *J. Phys. Oceanogr.*, 11, 324–336.

Lentz, S. J. (1995), The Amazon River plume during AMASSEDS: Subtidal current variability and the importance of wind forcing, *J. Geophys. Res.*, *100*, 2377-2390.

Li, Y., W. D. Nowlin, Jr., and R. O. Reid (1997), Mean hydrographic fields and their interannual variability over the Texas-Louisiana continental shelf in spring, summer, and fall, *J. Geophys. Res.*, *102*, 1027-1049.

Murray, S. P., E. Jarosz, and E. T. Weeks (1998), Physical oceanographic observations of the coastal plume, In: Final report: an observational study of the Mississippi-Atchafalaya coastal plume, OCS Study MMS 98-0040, U.S. Dept. of the Interior, MMS, Gulf of Mexico OCS Region, New Orleans, LA.

Murray, S. P., E. Jarosz, and E.T . Weeks (2001), Velocity and transport characteristics of the Louisiana-Texas Coastal Current, OCS Study MMS 2001-093, U.S. Dept. of the Interior, MMS, Gulf of Mexico OCS Region, New Orleans, LA.

Münchow, A. and R. W. Garvine (1993), Buoyancy and wind forcing of a coastal current, *J. Mar. Res.*, *51*, 293–322.

North, G. R., T. L. Bell, R. F. Cahalan, and F. J. Moeng (1982), Sampling errors in the estimation of empirical orthogonal functions, *Mon. Wea. Rev.*, *110*, 699–706.

Nowlin, W. D., Jr., A. E. Jochens, R. O. Reid, and S. F. DiMarco (1998), Texas-Louisiana Shelf circulation and transport processes study: Synthesis report, vol.1, Technical report, OCS Study MMS 98-0035, U.S. Dept. of the Interior, MMS, Gulf of Mexico OCS Region, New Orleans, LA.

Nowlin, W. D., Jr., A. E. Jochens, S. F. DiMarco, R. O. Reid, and M. K. Howard (2005), Low-frequency circulation over the Texas-Louisiana continental shelf, in *New Developments in the Circulation of the Gulf of Mexico*, W. Sturges and A. Lugo-Fernandez, Eds., AGU Monograph Series.

Oey, L. Y. (1995), Eddy and wind-forced shelf circulation, *J. Geophys. Res.*, *100*, 8621-8637.

Ohlmann, J. C., P. P. Niiler, C. A. Fox, and R. R. Leben (2001), Eddy energy and shelf interactions in the Gulf of Mexico, *J. Geophys. Res.*, 106, 2605–2620.

Sciremammano, F., Jr. (1979), A suggestion for the presentation of the correlations and their significance levels, *J. Phys. Oceanogr.*, 9, 1273–1276.

Smith, N. P. (1975), Seasonal variations in near shore circulation in the northwestern Gulf of Mexico, *Cont. Mar. Sci.*, *19*, 49–65.

Smith, N. P. (1978), Low-frequency reversals of near shore currents in the northwestern Gulf of Mexico, *Cont. Mar. Sci.*, *21*, 103–115.

Vastano, A. C., C. N. Barron, Jr., and E.W. Shaar Jr. (1995), Satellite observations of the Texas current, *Cont. Shelf Res.* *15*, 729–754.

Walker, N. D. (2005), Seasonal changes in surface temperature, shelf and slope circulation, and coastal upwelling in the northwestern Gulf of Mexico, in *New Developments in the Circulation of the Gulf of Mexico*, W. Sturges and A. Lugo-Fernandez, Eds., AGU Monograph Series.

Wang, W., W. D. Nowlin, Jr., and R. O. Reid (1998), Analyzed surface meteorological fields over the northwestern Gulf of Mexico for 1992–94: mean, seasonal and monthly patterns, *Mon. Wea. Rev.* *126*, 2864–2883.

Wiseman, W. J., Jr., R. E. Turner, F. J. Kelly, L. J. Rouse, Jr., and R. F. Shaw (1986), Analysis of biological and chemical associations near a turbid coastal front during winter 1982, *Contributions in Marine Science*, *29*, 141–151.

Wiseman, W. J., Jr., and F. J. Kelly (1994), Salinity variability within the Louisiana coastal current during the 1982 flood season, *Estuaries*, *17*, 732–739.

Wiseman, W.J., Jr., and F.J. Kelly (1995), Plumes and coastal currents near large river mouths, *Estuaries*, *18*, 509–517.

Wiseman, W. J., Jr., N. N. Rabalais, R. E. Turner, S. P. Dinnel, and A. MacNaughton (1997), Seasonal and interannual variability within the Louisiana coastal current: stratification and hypoxia, *J. Mar. Sys.*, *12*, 237–248.

Zavala-Hidalgo, J., S. L. Morey, and J. J. O'Brien (2003), Seasonal circulation on the western shelf of the Gulf of Mexico using high-resolution numerical model, *J. Geophys. Res.*, *108*, doi:10.1029/2003JC001879.

E. Jarosz, Oceananography Division (Code 7332), Naval Research Laboratory, Stennis Space Center, MS 39529, USA. (ewa.jarosz@nrlssc.navy.mil)

S. P. Murray, Office of Naval Research, 800 N. Quincy St., Arlington, VA 22217, USA. (MURRAYS@ONR.NAVY.MIL)